sustainability

MDPI

Article

Evaluating and Optimizing Air Quality Forecasting for Critical Particulate Matter Episodes in the Santiago Metropolitan Region, Chile

Luis Alonso Díaz-Robles [1], Marcelo Oyaneder [1], Julio López [1], Ariel Meza [1], Serguei Alejandro-Martin [2], Rasa Zalakeviciute [3], Diana Yánez [4], Andrea Espinoza-Pérez [5,6], Lorena Espinoza-Pérez [5,7], Ernesto Pino-Cortés [8] and Fidel Vallejo [1,9,*]

[1] Environmental Engineering and Management Particulas SpA, Santiago 7500010, Chile; luisdiazrobles@particulas.cl (L.A.D.-R.); marcelo.oyaneder@particulas.cl (M.O.); julio.lopez@particulas.cl (J.L.); ariel.meza@particulas.cl (A.M.)
[2] Department of Process Engineering and Bioproducts, Faculty of Engineering, Universidad del Bío-Bío, Concepción 4030000, Chile; salejandro@ubiobio.cl
[3] Biodiversidad, Medio Ambiente y Salud (BIOMAS), Universidad de Las Americas, Quito 170513, Ecuador; rasa.zalakeviciute@udla.edu.ec
[4] Agroindustrial Engineering, National University of Chimborazo, Riobamba 060108, Ecuador; estefania.yanez@unach.edu.ec
[5] Industrial Engineering Department, University of Santiago of Chile, Santiago 9170124, Chile; andrea.espinozap@usach.cl (A.E.-P.); lorena.espinozap@usach.cl (L.E.-P.)
[6] Program for the Development of Sustainable Production Systems (PDSPS), University of Santiago of Chile, Santiago 9170124, Chile
[7] Équipe de Recherche sur les Processus Innovatifs, Université de Lorraine (ERPI), 54000 Nancy, France
[8] Escuela de Ingeniería Química, Pontificia Universidad Católica de Valparaíso, Valparaíso 2362854, Chile; ernesto.pino@pucv.cl
[9] Industrial Engineering, National University of Chimborazo, Riobamba 060108, Ecuador
* Correspondence: fidel.vallejo@unach.edu.ec

Abstract

Severe wintertime particulate pollution (PM_{10} and $PM_{2.5}$) affects the Santiago Metropolitan Region in Chile and is intensified by basin topography and frequent thermal inversions. Local authorities rely on the Critical Episodes Management (CEM) forecasting system, yet its predictive performance is variable. This study assesses CEM to identify operational vulnerabilities and propose data-driven improvements for urban air-quality governance. About ~1.2 million hourly meteorological and air-quality records (2017–2022) were analyzed using Generalized Additive Models (GAMs) to characterize key nonlinear relationships, and we evaluated the operational skill of the Cassmassi-1 PM_{10} model and the WRF-Chem-based $PM_{2.5}$ forecasting component used by the system. Cassmassi-1 missed more than 50% of critical episodes and showed a false-alarm rate above 60%, consistent with limitations associated with static or incomplete emission representations. By contrast, the WRF-Chem-based component achieved episode prediction accuracy above 70%. GAM results indicate that wind speeds below 2 m s^{-1}, high diurnal temperature range, and relative humidity below 65% are strongly associated with extreme events. Considering the results, we recommend transitioning to nonlinear forecasting approaches that explicitly incorporate these meteorological thresholds and vertical stability indicators to improve alert reliability, strengthen urban resilience, and reduce population exposure.

Keywords: air quality forecasting; particulate matter; thermal inversion; urban sustainability; Santiago de Chile

Check for updates

Academic Editor: Luca Stabile

Received: 9 March 2026
Revised: 1 April 2026
Accepted: 3 April 2026
Published: 8 April 2026

1. Introduction

Air pollution remains a significant environmental challenge for sustainable urban development worldwide, posing substantial risks to public health and urban resilience [1,2]. In the Global South, rapidly growing cities frequently struggle to harmonize economic growth with environmental sustainability [3]. The Santiago Metropolitan Region (SMR) in Chile serves as a prime example of this conflict. For many years, the SMR has faced persistent air quality challenges, primarily due to elevated levels of fine ($PM_{2.5}$) and coarse particulate matter (PM_{10}), especially during the austral autumn and winter seasons [4–6].

The environmental crisis in Santiago de Chile is primarily attributed to the region's intricate orography and prevailing meteorological conditions [7]. The city is situated within an enclosed basin, bordered by the Andes Mountains to the east and the coastal mountain range to the west. This geographical configuration limits both horizontal and vertical dispersion, resulting in the systematic accumulation of pollutants, particularly under stable boundary-layer conditions [8,9]. This topographical confinement is exacerbated by seasonal meteorological phenomena, such as persistent thermal inversions, shallow mixing layers, and atmospheric subsidence driven by the South Pacific Subtropical Anticyclone, which facilitate prolonged episodes of elevated particulate matter concentrations. Observational and modeling studies have documented these dynamics, highlighting the correlation between a reduced boundary-layer height, weak ventilation coefficients, and significant increases in particulate matter levels during stagnant conditions [10].

Human-induced emission sources markedly intensify the influence of these natural constraints. Residential wood combustion is a leading source, contributing approximately 78% of total $PM_{2.5}$ emissions in the SRM [11]. The resultant particulate matter concentrations frequently surpass the national primary air quality standards (20 $\mu g\ m^{-3}$ annually and 50 $\mu g\ m^{-3}$ over a 24 h period), which were designed to protect public health. This persistent non-compliance highlights a critical vulnerability, as prolonged exposure to fine particulate matter in the region is closely linked to heightened cardiovascular and respiratory morbidity and increased overall disease burden [12,13].

Chile has positioned itself as a frontrunner in Latin America for addressing systemic environmental issues through the implementation of regional air quality regulations. Among these nationwide efforts, Santiago's regulatory framework remains the longest-standing and most extensively updated. First introduced in 1996 and significantly updated in 2017, the SMR plan underscores the scale of the national pollution crisis and the ongoing efforts to achieve sustainable development [14].

To anticipate and mitigate extreme pollution events each year, Chile's environmental authorities operate the Critical Episodes Management (CEM) system from May to August. This preventive framework relies on the hourly Particulate Matter Index (PMI) to classify air quality into Alert, Pre-emergency, and Emergency levels (Table 1). Reaching these predefined thresholds triggers immediate interventions, such as vehicular restrictions, bans on residential wood heating, and the temporary suspension of high-emitting industries, all aimed at protecting public health.

Table 1. PMI thresholds for the CEM system.

Critical Episode Level	$PM_{2.5}$ ($\mu g\ m^{-3}$)	PM_{10} ($\mu g\ m^{-3}$)
Alert	80–109	180–229
Pre-emergency	110–169	230–329
Emergency	$\geq$170	$\geq$330

Past crises have clearly demonstrated the imperative for accurate predictive systems. For instance, the 2018 Quintero-Puchuncaví episode, where mass intoxications occurred

https://doi.org/10.3390/su18083652

due to unforecasted spikes in $PM_{2.5}$, sulfur dioxide (SO_2), and volatile organic compounds (VOCs), exposed the severe vulnerabilities associated with inadequate predictive modeling [15]. Similarly, extreme $PM_{2.5}$ events in the SMR during 2015–2016, with concentrations peaking at 300 μg m^{-3} under adverse meteorological conditions, further emphasized the critical need for resilient, proactive management frameworks [16].

Air quality modeling in SMR is inherently complex due to the nonlinear interactions between anthropogenic emissions and meteorological variables such as wind speed, temperature, relative humidity, and thermal inversions. The CEM system has historically relied on the Cassmassi-1 model [17] to forecast PM_{10} episodes in SMR and the Weather Research and Forecasting with Chemistry (WRF-Chem) model to predict $PM_{2.5}$ concentrations [18]. However, both frameworks face significant challenges in structural modeling. The statistical Cassmassi-1 model struggles to capture nonlinear atmospheric dynamics and lacks the capacity to incorporate dynamic anthropogenic emission inventories. Conversely, while WRF-Chem integrates complex emission data, its prognostic accuracy in the basin is fundamentally constrained by the absence of dedicated high-altitude atmospheric soundings required to resolve the thermal inversion layer accurately.

Beyond these structural modeling challenges, the limitations of the CEM are further exacerbated by variable data quality. For instance, between 2017 and 2022, stations such as Quilicura and Cerrillos experienced a 100% data loss for $PM_{2.5}$ and PM_{10}, whereas stations like Pudahuel, Cerro Navia, and El Bosque recorded less than 10% of missing data. These crucial data gaps, combined with the systematic underestimation of key variables such as wind speeds dropping below 2 m s^{-1} in 80% of undeclared events and relative humidity falling under 65% in 75% of cases, underscore the urgent need to overhaul the forecasting framework.

Consequently, this study represents the first comprehensive performance assessment of the CEM system in the Santiago Metropolitan Region in decades, covering the period 2017–2022. Its primary objectives are to validate the system's predictive accuracy, identify systematic biases in the forecasting of critical episodes, and propose targeted, data-driven improvements to the CEM framework based on a thorough analysis of air quality and meteorological variables. These enhancements are intended not only to strengthen preventive pollution management and ensure stricter regulatory compliance but also to modernize the forecasting system, providing a valuable tool for anticipating critical episodes, reducing population exposure, and strengthening urban environmental resilience.

2. Materials and Methods

2.1. Data Acquisition and Preprocessing

To evaluate the performance of the Critical Episodes Management (CEM) forecasting system in the Santiago Metropolitan Region, air quality and meteorological data were collected for the winter management periods (1 May to 31 August) from 2017 to 2022. Hourly concentrations of $PM_{2.5}$ and PM_{10} were retrieved from the 11 monitoring stations of the National Air Quality Information System (SINCA in Spanish) operated by the Chilean Ministry of the Environment. The meteorological variables included wind speed, wind direction, relative humidity and air temperature. All data were obtained directly from the publicly accessible SINCA database.

In addition, hourly temperature records from three altitudinal stations of the Dirección Meteorológica de Chile (DMC)—Lo Prado (1068 m asl), San Pablo (482 m asl), and Quinta Normal (517 m asl)—were incorporated to calculate vertical temperature gradients and identify thermal inversion episodes. Figure 1 shows the spatial distribution of the monitoring stations used in this study.

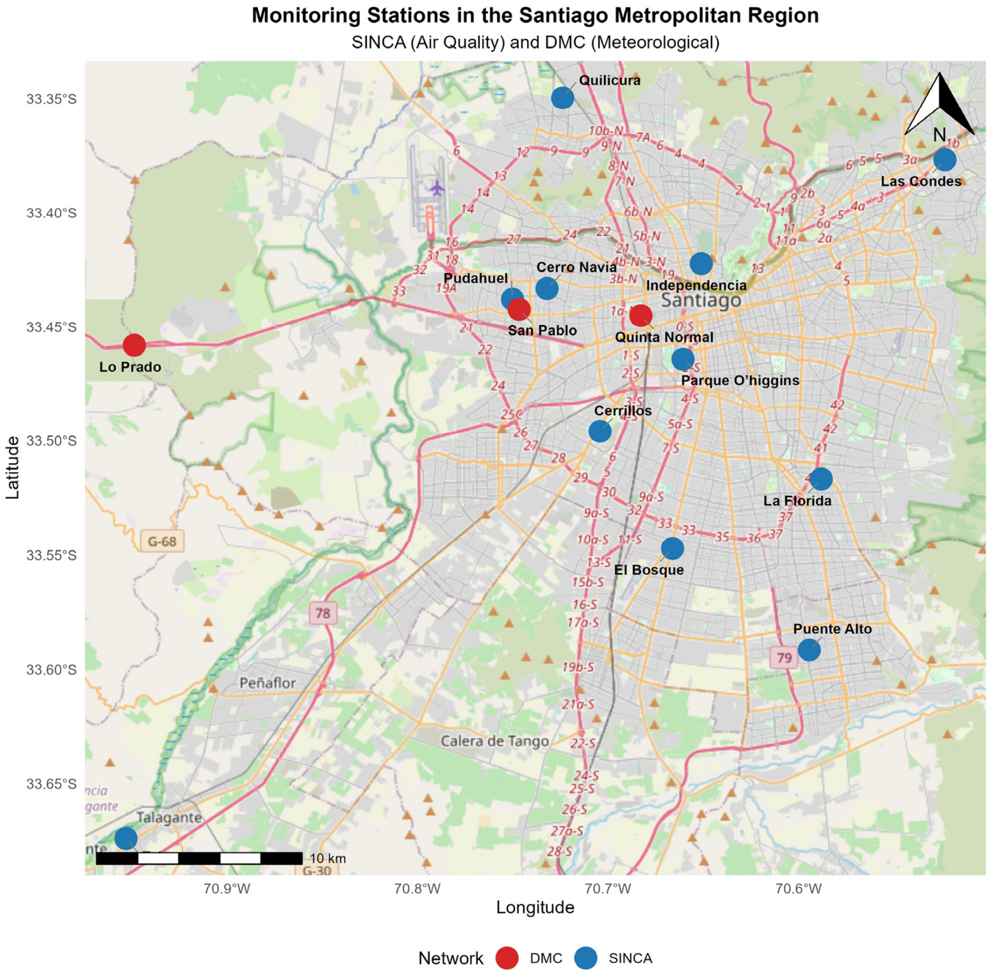

Figure 1. Location of air quality monitoring stations from the SINCA network (blue) and meteorological stations from the DMC network (red) in the Santiago Metropolitan Region.

A total of approximately 1.2 million hourly records were compiled across six years. Rigorous data quality control was applied to ensure reliability. First, a completeness threshold of 50% was established: any monitoring station with more than 50% missing values for $PM_{2.5}$, PM_{10}, or the main meteorological variables during the study period was excluded from subsequent statistical analyses and model evaluations. This specific criterion was selected because interpolating more than half of a time series would introduce unacceptable synthetic bias, compromising the detection of nonlinear meteorological thresholds and rendering the evaluation of operational false negatives statistically invalid. As a result, stations such as Quilicura (V) and Cerrillos (P) were completely removed because they presented 100% data loss across all six years (see Table 2 for detailed missing-data percentages per station and year).

The remaining stations underwent standardized preprocessing procedures in accordance with official SINCA protocols. These steps included: (i) detection and removal of physically implausible values and outliers using the interquartile range method (values outside 1.5 × IQR), (ii) correction of format inconsistencies (e.g., time-stamp alignment and unit standardization), and (iii) linear interpolation for short gaps (<3 consecutive hours) when justified. After preprocessing, four high-quality stations with the lowest missing-data rates—Independencia (F), Cerro Navia (R), Pudahuel (O), and El Bosque (Q)—were selected for the core statistical modeling (Pearson correlations and Generalized Additive Models) because they provided continuous and representative coverage of the western and central sectors of the basin, where the highest frequency of critical episodes occurs.

Table 2. Percentage of missing meteorological data for each monitoring station in the Santiago Metropolitan Region during the winter periods (May–August) from 2017 to 2022.

Monitoring Station (Code)	2017 (%)	2018 (%)	2019 (%)	2020 (%)	2021 (%)	2022 (%)
Independencia (F)	1.36	0.73	0.2	0.18	21	100
La Florida (L)	16.15	2.82	0	0.09	0	1.37
Las Condes (M)	64.58	54.26	0	0	0.01	0.45
Parque O'Higgins (N)	0	3.42	0	0	0.8	0.03
Pudahuel (O)	4.29	1.68	1.05	0.03	0	0.1
Cerrillos (P)	100	100	100	100	100	100
El Bosque (Q)	0.1	32.76	0.44	0.76	0.08	0.03
Cerro Navia (R)	0.91	5.12	0	0.57	0.19	16.85
Puente Alto (S)	25.4	13.76	0	2.54	0.08	1.18
Talagante (T)	0.09	13.72	0.39	100	100	1.09
Quilicura (V)	100	100	100	100	100	100

This preprocessing pipeline ensured a robust, consistent dataset while preserving the operational nature of the evaluation. All data handling and quality-control steps were performed in R (v. 4.3.2).

2.2. Evaluation of the Operational Forecasting System

To systematically evaluate the Critical Episodes Management (CEM) forecasting system, all air quality events recorded between 2017 and 2022 were classified into two mutually exclusive categories:

- Declared events: Days officially registered within the CEM system as Alert, Pre-emergency, or Emergency, based on the forecasted $PM_{2.5}$ and PM_{10} thresholds.
- Undeclared events: False negative occurrences where observed particulate matter concentrations exceeded regulatory thresholds, yet no critical episode was forecasted or officially declared.

The CEM system operationally employs two distinct forecasting models: the Cassmassi-1 model, a multiple linear regression approach that uses categorical meteorological conditions and persistence of previous concentrations to predict PM_{10} episodes, and the WRF-Chem model, a fully coupled online chemistry-transport model that incorporates anthropogenic and natural emission inventories to forecast $PM_{2.5}$ concentrations. No additional variable selection or hyperparameter tuning was performed, as the study evaluates the operational configuration used by the authorities.

For declared events, contingency tables were constructed to compare forecasted air quality categories with observed conditions. For undeclared events, a retrospective analysis of meteorological preconditions (e.g., wind speed at 18:00 h and relative humidity at 12:00 h of the preceding day) was conducted to identify missing predictive patterns and precursor variables that the current operational models failed to capture. Classification metrics focused on episode detection (Precision, Recall, and F1-score) were calculated for the binary outcome ("No Episode" versus "Episode"). Precision was defined as TP/(TP + FP), Recall as TP/(TP + FN), and F1-score as the harmonic mean of Precision and Recall, where TP, FP, and FN correspond to true positives, false positives, and false negatives for critical episodes, respectively. The original detailed contingency tables are provided in the Supplementary Material.

2.3. Statistical Analysis and Modeling

Statistical analyses were designed to uncover nonlinear relationships between meteorological variables and particulate matter concentrations, to propose data-driven improvements to the existing models. Preliminary data manipulation, cleaning, and filtering were performed.

To explore the complex, nonlinear dynamics inherent to atmospheric pollution in the basin, Generalized Additive Models (GAMs) were used [19,20]. This approach is highly suitable for meteorological datasets where traditional linear assumptions fall short. Statistical modeling and contingency matrix validations were executed in R [21]. A recognized limitation of this methodology is the reliance on surface-level meteorological data, as the absence of vertical atmospheric soundings restricts the complete characterization of thermal inversion layers.

Figure 2 summarizes the complete methodological workflow applied in this study. The framework integrates five analytical stages: data acquisition and quality control (Section 2.1), episode classification into declared and undeclared events (Section 2.2), statistical modeling via GAMs with stepwise variable selection (Section 2.3), independent evaluation of the operational forecasting models (Cassmassi-1 and WRF-Chem), and the derivation of performance metrics to support data-driven recommendations for the CEM system. This structured workflow was designed to ensure transparency and reproducibility, allowing each analytical decision to be traced back to an explicit methodological step.

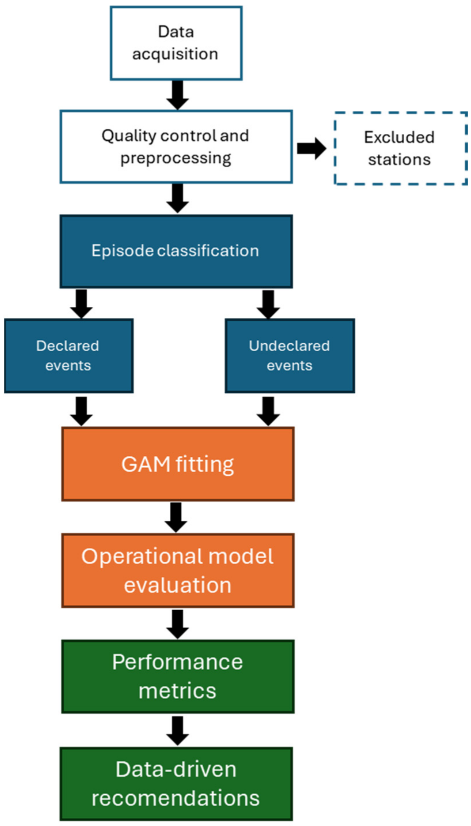

Figure 2. Methodological workflow of the study.

3. Results

3.1. Data Availability and Quality Assessment

Prior to evaluating the forecasting models, a comprehensive assessment of SINCA's meteorological data availability was conducted for 11 stations. Table 2 summarizes the annual percentage of missing meteorological data for each station between 2017 and 2022. As observed in the data consistency analysis, stations such as Quilicura and Cerrillos experienced 100% data loss across the entire six-year study period. Furthermore, stations like Talagante and Independencia exhibited complete data loss in specific recent years.

Consequently, in alignment with the established methodological thresholds, stations lacking sufficient and continuous data representations were strictly excluded from subsequent forecasting evaluations and statistical modeling to ensure the robustness of the results.

3.2. Current Status of the Critical Episodes Management System

Between 2017 and 2022, a total of 48 critical episodes were officially declared by environmental authorities under the CEM framework, averaging 8 per year. However, observational data from the monitoring network reveal a broader temporal distribution of $PM_{2.5}$ threshold exceedances. As detailed in Table 3, a total of 172 critical $PM_{2.5}$ events (both declared and undeclared) were recorded during the winter management periods over the six years.

Table 3. Number of observed critical $PM_{2.5}$ episodes in SMR by month from 2017 to 2022.

Month	2017	2018	2019	2020	2021	2022	Total	%
May	5	7	3	1	4	6	26	15.1
June	10	17	12	4	8	10	61	35.5
July	9	10	16	11	18	3	67	39.0
August	3	5	3	1	6	0	18	10.4

The highest frequency of these episodes occurred in July, accounting for 39.0% of the events (67 episodes), followed by June with 35.5% (61 episodes). The transitional months of May and August recorded significantly lower frequencies, representing 15.1% (26 episodes) and 10.4% (18 episodes), respectively.

3.3. Spatial Distribution of Critical Episodes

The spatial distribution of critical episodes reveals marked disparities across the stations. Figures 3 and 4 show the observed PM_{10} and $PM_{2.5}$ episodes per year, respectively. The monitoring stations located in the lower western areas of Santiago, specifically Pudahuel and Cerro Navia, recorded the highest frequency of critical events. During the study period, Pudahuel reported 39 and 15 episodes of PM_{10} and $PM_{2.5}$, respectively, while Cerro Navia reported 38 and 12, respectively.

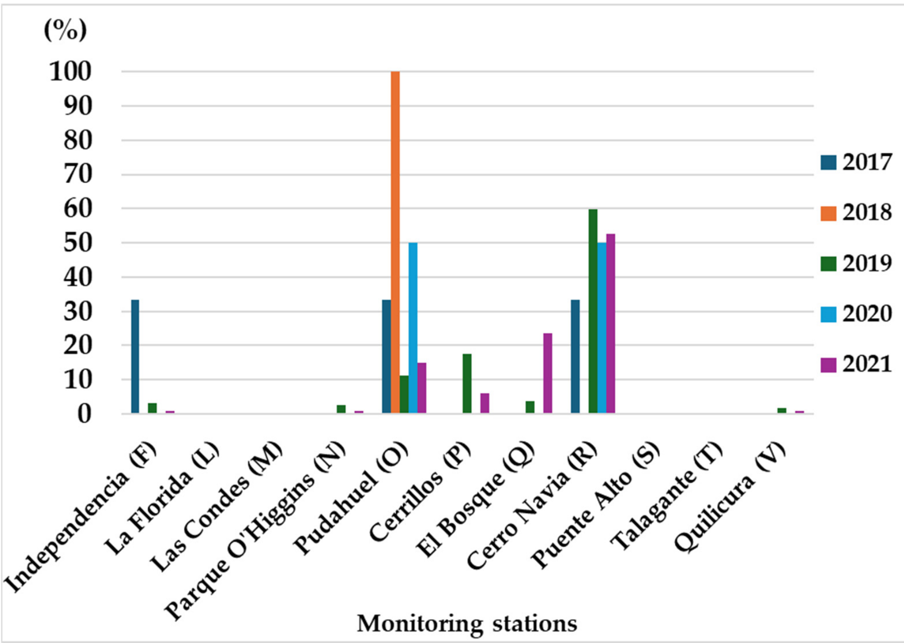

Figure 3. Distribution of critical PM_{10} episodes per year.

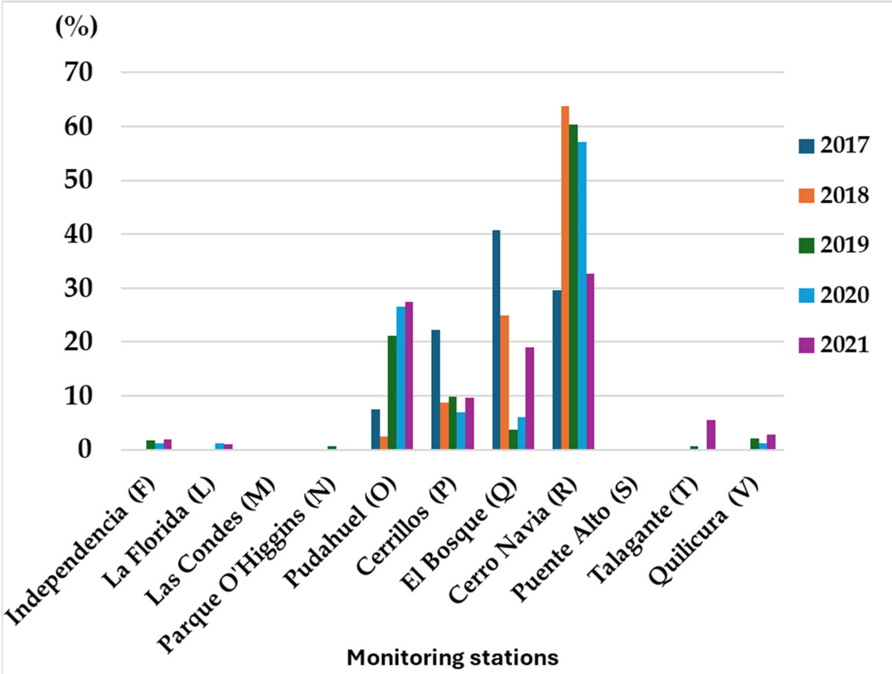

Figure 4. Distribution of critical $PM_{2.5}$ episodes per year.

Conversely, monitoring stations situated closer to the foothills of the Andes Mountains, such as Las Condes and La Florida, exhibited a significantly lower occurrence of critical episodes. Las Condes, for instance, recorded only three PM_{10} and two $PM_{2.5}$ episodes.

3.4. Evaluation of CEM Performance and Undeclared Episodes

Predictive models for critical episode management face a fundamental trade-off: achieving sufficient accuracy to prevent undetected high-pollution events while simultaneously minimizing excessive false alarms that could undermine public compliance and resource efficiency. In this context, it is also pertinent to note that the predictive model itself inherently influences the predicted air quality, as the declaration of critical episodes (alert, pre-emergency, or emergency) triggers emission control measures that alter actual pollutant concentrations, thereby introducing feedback between the forecast and the observed outcome. This interdependence highlights the challenge of evaluating model performance in an operational setting where interventions are conditional on the predictions.

Between 2017 and 2022, 12 undeclared episodes were identified, those instances in which ambient concentrations exceeded regulatory thresholds without prior activation of preventive measures. These included a major PM_{10} event on 29 June 2022, and seven $PM_{2.5}$ cases clustered between 2020 and 2021.

These unforecasted events, primarily recorded at the Pudahuel and Cerro Navia stations, were strongly associated with a specific set of meteorological preconditions: wind speeds below 2 m s^{-1} in 80% of the cases, relative humidity under 65% in 75% of the cases, and temperature ranges strictly between 11 and 14 °C in 70% of the occurrences. These forecasting failures strongly suggest that key meteorological variables governing surface atmospheric stability and regional subsidence are either being underestimated or inadequately represented within the current linear models of the CEM system. This underscores the urgent need to integrate these specific meteorological parameters into more robust, nonlinear predictive frameworks.

3.5. Statistical Modeling of Meteorological Variables: Correlations and Generalized Additive Models

To evaluate the limitations of the current CEM forecasting system and propose data-driven improvements, a comprehensive statistical analysis was conducted on 1.2 million hourly records from four high-quality stations: Independencia, Cerro Navia, Pudahuel, and El Bosque. The analysis evaluated the relationship between particulate matter and key meteorological drivers, including average wind speed, minimum temperature, average relative humidity, and diurnal temperature range (DTR), the difference between daily maximum and minimum temperatures.

Figure 5 presents the Pearson correlation coefficients for the selected stations. Average wind speed demonstrated the highest statistical significance across all sites, exhibiting negative correlation coefficients ranging from −0.65 to −0.78 for $PM_{2.5}$ and from −0.58 to −0.72 for PM_{10}. This inversely proportional relationship is consistent with the dilution effect documented in previous basin-dynamics studies [1,2]. For instance, in Pudahuel, the correlation between wind speed and $PM_{2.5}$ reached −0.78 ($p < 0.01$), underscoring the critical role of ventilation in pollutant dispersion.

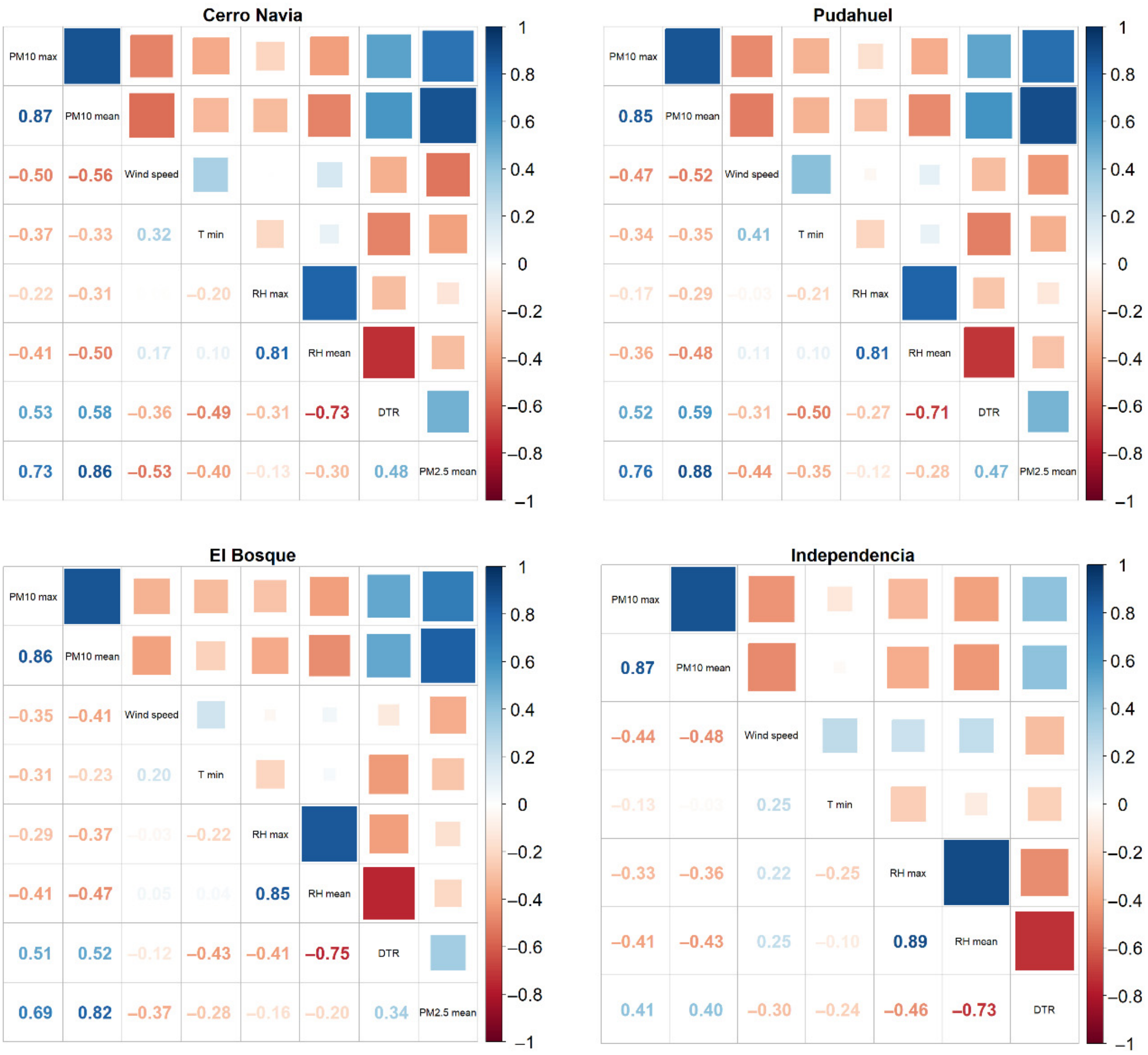

Figure 5. Pearson correlation coefficients between meteorological variables and $PM_{2.5}/PM_{10}$ concentrations at selected stations in the Santiago Metropolitan Region.

DTR exhibited positive correlations with PM_{10} exceeding 0.50 at Cerro Navia, Pudahuel, and El Bosque ($p < 0.05$). This suggests that pronounced temperature variations, typically associated with strong winter thermal inversions, limit the development of the mixing layer and facilitate pollutant accumulation [22]. Conversely, daily minimum temperature and average relative humidity showed weak or non-significant linear correlations ($r < 0.30$, $p > 0.05$). However, the low linear significance of variables such as humidity often masks complex, threshold-dependent interactions that require nonparametric approaches to be properly captured [23].

To overcome the limitations of linear assumptions, GAMs were constructed using cubic splines to capture the nonlinear dynamics between PM concentrations and meteorological variables. As illustrated in Figure 6, the GAMs successfully explained between 60% and 75% of the variance for $PM_{2.5}$ and between 55% and 70% for PM_{10}, yielding highly significant adjusted R^2 values ($p < 0.01$).

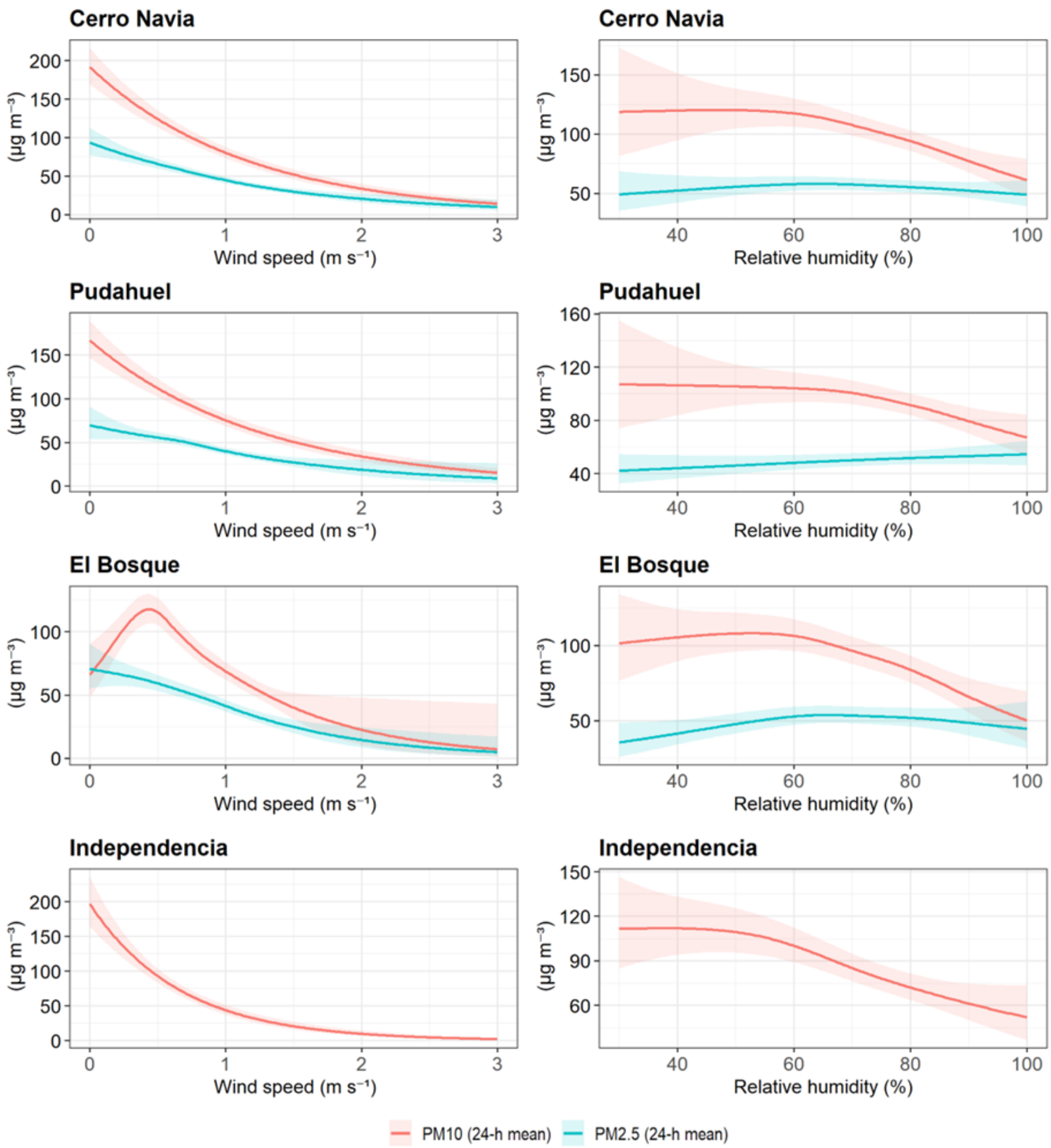

Figure 6. Generalized Additive Model (GAM) smooth functions illustrating the nonlinear relationships between selected meteorological variables and $PM_{2.5}/PM_{10}$ concentrations at representative monitoring stations in the Metropolitan Region.

The models showed a steep, nonlinear decline in $PM_{2.5}$ and PM_{10} concentrations as wind speeds exceeded 2 m s^{-1}. In Pudahuel, the GAMs indicated that an increase in wind speed from 1 to 3 m s^{-1} reduced $PM_{2.5}$ concentrations by an average of 40%. Furthermore, relative humidity exhibited distinct threshold-dependent behaviors. In Cerro Navia, PM_{10} concentrations increased slightly with humidity up to 65%, but decreased by 15% when humidity exceeded this threshold. This pattern likely reflects the dual role of humidity in aerosol dynamics, where moderate moisture promotes particle growth, while high humidity leads to wet deposition and sedimentation [24].

Thermal inversions were evaluated by analyzing temperature differentials between altitudinal stations at Lo Prado at 1068 m above sea level (asl) versus San Pablo and Quinta Normal at 482–517 m asl. Figures 7 and 8 show the results for maximum $PM_{2.5}$ and PM_{10} at each hour of the day, for both the thermal-inversion and no-thermal-inversion scenarios, using all data from 2020, 2021, and 2022.

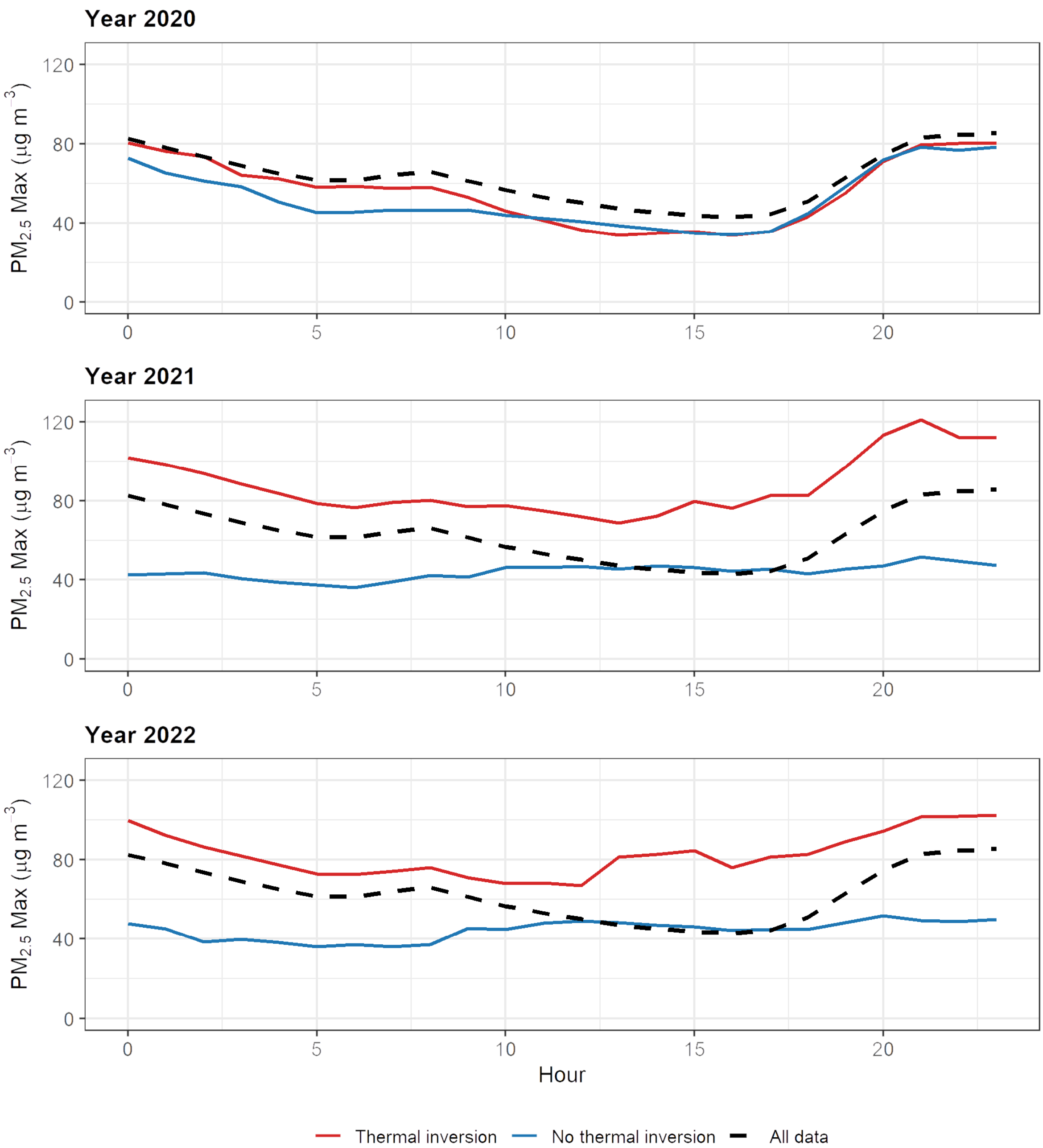

Figure 7. Hourly maximum $PM_{2.5}$ concentrations averaged over the years 2020–2022 at selected monitoring stations in the Metropolitan Region.

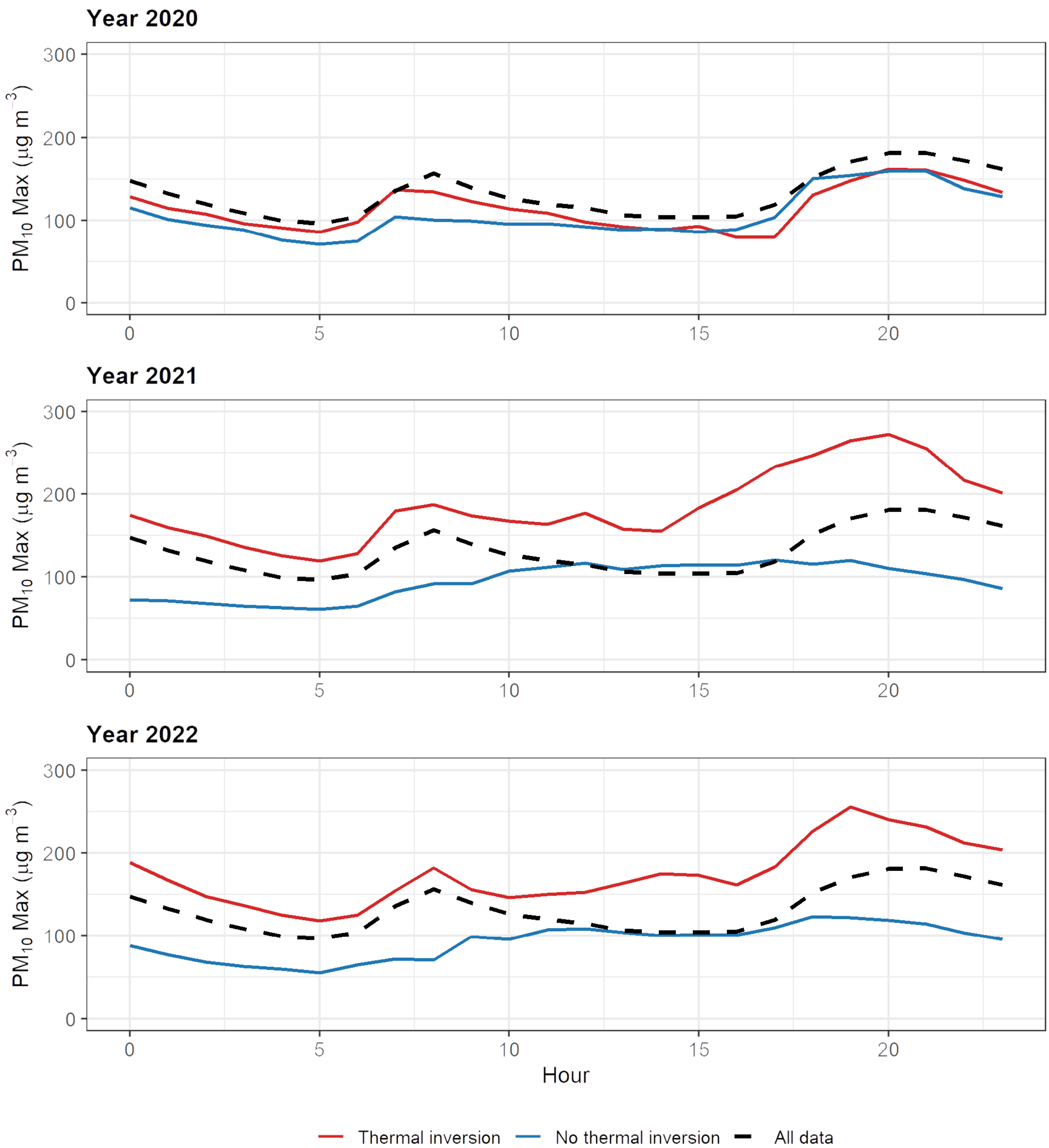

Figure 8. Hourly maximum PM_{10} concentrations averaged over the years 2020–2022 at selected monitoring stations in the Metropolitan Region.

As illustrated in Figures 7 and 8, with the notable exception of 2020, maximum PM_{10} and $PM_{2.5}$ concentrations remained consistently above the overall average on days characterized by thermal inversions. Conversely, on days without thermal inversions, particulate matter levels generally fell below the mean. The diurnal variability in pollution levels is primarily driven by fluctuations in near-surface atmospheric stability during the nocturnal period, coupled with the development of the mixing layer and its internal wind dynamics during the daytime. In this context, thermal inversions are a frequent meteorological phenomenon in the central valley of Chile. This structural feature largely explains the heightened pollution levels observed during the colder months, as it severely limits the vertical development of the mixing layer and weakens internal wind dispersion [9].

Anomalously, during 2020, the maximum concentrations of PM_{10} and $PM_{2.5}$ remained closely aligned with, or even below, the overall average on days with and without thermal inversions. This significant deviation is highly likely attributable to the drastic reduction in particulate matter emissions during the COVID-19 lockdowns, which altered the regular anthropogenic activity levels observed in subsequent years [25–27]. Indeed, the strict mandatory quarantine imposed on the Santiago Metropolitan Region began in May 2020 and concluded at the end of August, a timeframe that perfectly coincides with the critical episodes management period [28,29].

3.6. Performance Evaluation of the Operational Forecasting Models

To critically assess the efficacy of the Critical Episodes Management (CEM) system, the performance of the Cassmassi-1 model for PM_{10} and the WRF-Chem model for $PM_{2.5}$ was evaluated over the 2020–2022 period. It must be explicitly noted that this evaluation does not intend to perform a direct algorithmic benchmark between Cassmassi-1 and WRF-Chem, as they are fundamentally different models designed for different pollutants with distinct emission sensitivities. Rather, the objective is to independently evaluate the operational reliability of the two primary forecasting pillars upon which the authorities currently rely to protect public health.

The evaluation compared forecasted conditions against observed data, focusing not only on overall accuracy but also on key operational metrics, including false alarm rate and undeclared episode rate. In addition, classification metrics specifically suited to imbalanced events (Precision, Recall, and F1-score) were calculated to evaluate the models' ability to detect critical episodes. Results are summarized in Table 4.

Table 4. Performance of the models forecasting particulate matter during 2020–2022.

Model	Year	OA (%)	Acc NO (%)	Acc YES (%)	FA (%)	UE (%)	Precision	Recall	F1-Score
Cassmassi-1	2020	95.0	96.6	33.3	80.0	66.7	0.20	0.33	0.25
	2021	78.2	84.0	47.4	64.0	52.6	0.36	0.47	0.41
	2022	80.5	86.0	43.8	68.2	56.3	0.32	0.44	0.37
WRF-Chem	2020	78.5	80.8	64.7	64.5	35.3	0.35	0.65	0.46
	2021	79.0	81.9	72.2	36.6	27.8	0.63	0.72	0.67
	2022	86.2	86.5	84.2	46.7	15.8	0.53	0.84	0.65

OA: Overall Accuracy, Acc NO: Accuracy of "No Episode", Acc YES: Accuracy for critical episodes, FA: False Alarms, UE: Undeclared Episodes.

The Cassmassi-1 model for PM_{10} demonstrated high accuracy in predicting "No Episode" conditions, consistently exceeding 84% across the three years. However, its performance in detecting critical episodes was severely limited, with Recall values ranging from 0.33 to 0.47 and very low Precision (0.20–0.36). The model showed 0% accuracy in Pre-emergency conditions and produced false alarm rates above 60% annually. Consequently, it failed to alert authorities to more than 50% of the actual episodes each year. This critical deficiency is primarily due to the model's structural limitations; Cassmassi-1 relies heavily on meteorological conditions and cannot incorporate dynamic emission inventories [29], thereby ignoring the fact that PM_{10} concentrations are strongly driven by anthropogenic emissions [11].

Furthermore, temporal analysis revealed that July was the most challenging month for the model. This is likely due to the combination of the year's coldest temperatures, minimal ventilation, and a peak in residential wood heating. Similarly, the model struggled significantly on weekends and Mondays, failing to capture the emission spikes from weekend wood-burning and Monday-morning vehicular traffic.

In contrast, the WRF-Chem model for $PM_{2.5}$ showed a more robust, balanced performance. While it also achieved high accuracy for "No Episode" days (above 80%), it demonstrated substantially superior capacity to detect actual critical episodes, with Recall values ranging from 0.65 to 0.84 and F1-scores between 0.46 and 0.67. The rate of undeclared episodes remained below 27% across the three years, and the model successfully predicted more than 38% of monthly episodes and over half of the emergencies occurring on weekends and Mondays.

The superior performance of WRF-Chem is primarily due to its ability to integrate comprehensive anthropogenic and natural emission inventories, enabling it to better account for the chemical and dynamic processes driving $PM_{2.5}$ formation under complex basin conditions.

4. Discussion

The pronounced seasonal episodes with a high concentration of particulate matter shown in Table 3 are intrinsically linked to the colder, highly stable meteorological conditions characteristic of the austral winter. During these peak months, the Santiago basin experiences limited mixing-layer development and anomalously weak wind speeds, effectively stalling the atmospheric ventilation of the urban area [22]. Furthermore, the frequent occurrence of thermal inversions in the central Chilean valley during the winter period acts as a physical meteorological barrier, trapping anthropogenic emissions near the surface and significantly amplifying the accumulation of particulate pollutants [30]. The results here reinforce the idea that the geographic and climatic configuration of the Santiago basin creates highly unfavorable conditions for the dispersion of atmospheric pollutants, particularly during the austral winter.

The spatial variations observed in Figures 5 and 6 are largely attributable to topographical and meteorological factors. The lower-altitude western stations are more exposed to localized anthropogenic emissions and experience severe atmospheric stagnation typical of dense urban areas [9,31]. In contrast, the eastern foothill stations benefit from nocturnal mountain breezes that enhance local ventilation and disperse pollutants. Regardless of these spatial differences, a preliminary regulatory analysis indicates that daily $PM_{2.5}$ concentrations exceeded the 50 $\mu g/m^3$ threshold on at least 30 days per year in the most affected western stations, highlighting a systemic and ongoing breach of primary air quality standards across the basin.

The persistence of coastal lows, characterized by pronounced warming and drying above the thermal inversion layer, generates critical stagnation that severely limits the vertical development of the mixing layer and weakens internal wind dispersion. Within this context, diurnal variability in pollution levels is heavily dependent on nocturnal atmospheric stability and specific meteorological precursors. The results from the GAM revealed that wind speed and DTR are the most critical drivers of particulate matter accumulation. While minimum temperature alone was a weak predictor, a high DTR, indicative of a strong thermal inversion, coupled with relative humidity below 65% and nocturnal wind speeds below 2 m s^{-1}, directly exacerbates $PM_{2.5}$ and PM_{10} accumulation.

The GAM analysis highlights threshold-dependent behaviors with clear physical meaning and provides highly actionable operational insights. Wind speeds below 2 m s^{-1} represent a critical local ventilation threshold below which pollutant dilution becomes extremely inefficient, leading to rapid accumulation. Similarly, relative humidity below 65% favors particle growth and reduces wet deposition, while high diurnal temperature ranges strengthen thermal inversions and suppress mixing-layer development. These quantified nonlinear relationships explain exactly when and why linear models such as Cassmassi-1 struggle to anticipate extreme events, offering local authorities specific empirical triggers to identify potential false negatives.

From an environmental and public health perspective, the poor performance of the Cassmassi-1 model has significant consequences. The high rate of undeclared episodes (>50%) indicates that preventive measures are often not activated when pollution levels are most harmful, resulting in unnecessary population exposure to elevated PM concentrations.

Conversely, persistently high false alarm rates (>60%) can lead to alert fatigue, reduced public compliance, and inefficient use of regulatory resources. These limitations undermine the effectiveness of the current early warning system and weaken the overall air quality management framework in the Santiago Metropolitan Region.

The findings of this study, therefore, have direct implications for public policy. Improving the reliability of critical episode forecasting is essential to strengthening the Preventive Plan and better protecting public health. Incorporating nonlinear approaches and key precursor variables (such as evening wind deceleration and midday humidity drops) into the operational system would enhance alert accuracy, increase public trust, and support more timely and targeted emission control measures.

Despite the complex, nonlinear relationship between pollution levels and these meteorological and anthropogenic variables, the current CEM system relies heavily on qualitative assessments and linear forecasting models, leading to significant predictive vulnerabilities. Evaluating the operational models between 2020 and 2022 revealed that the Cassmassi-1 model for PM_{10} failed to predict more than 50% of critical episodes and generated a false alarm rate exceeding 60%. This deficiency stems largely from its inability to incorporate dynamic emission inventories. The Cassmassi-1 model [17], based on a multiple linear regression approach, has been historically applied to forecast PM_{10} episodes in Chile. However, alternative statistical approaches, such as log-linear models based on asymmetric distributions, have been proposed to capture better the extreme nature of these episodes [32].

Effective implementation of these advanced models demands robust vertical atmospheric datasets, particularly temperature and wind profiles, which remain limited in the SMR owing to the scarcity of routine high-altitude soundings. Consequently, the operational CEM forecasting system relies on surface observations from stations at varying elevations to estimate tropospheric conditions, thereby introducing notable uncertainties in the physical representation of the mixing layer height and subsidence processes [9].

Conversely, the WRF-Chem model for $PM_{2.5}$ demonstrated superior performance, achieving an accuracy above 70% in episode prediction and reducing undeclared episodes to under 27%, directly benefiting from the integration of anthropogenic and natural emission data.

The nonlinear relationships and critical thresholds identified through the GAM analysis highlight the structural limitations of current linear approaches [33]. While developing and validating a new operational forecasting tool is beyond the scope of this diagnostic study, our findings suggest that future predictive frameworks must explicitly incorporate these nonlinear dynamics. These systems should explicitly integrate specific temporal precursors, such as wind speed decreases starting at 18:00 h and relative humidity drops from 12:00 h. Finally, addressing the structural lack of vertical atmospheric data is imperative; estimating thermal inversions through altitudinal surface stations introduces critical uncertainties. Deploying dedicated high-altitude atmospheric soundings to measure the vertical temperature profile quantitatively is an essential step toward building a more resilient and precise air quality forecasting system.

On the other hand, this study has several limitations that should be acknowledged. First, due to strict data completeness criteria, stations with more than 50% missing data (such as Quilicura and Cerrillos) were excluded, potentially introducing selection bias toward better-maintained stations located mainly in the western and central parts of the basin. Second, the quantitative evaluation of model performance was limited to the 2020–2022 period due to the availability of official forecast records. Third, the assessment of thermal inversions relied exclusively on surface temperature differences between altitudinal stations, as routine high-altitude soundings are unavailable; this approach introduces significant representativeness uncertainty into the characterization of boundary-layer stability and other processes critical to extreme pollution episodes. Furthermore, this study inherently relies on observational data from a public monitoring network, which carries unquantified measurement uncertainties and potential calibration drifts over the six years. Finally, although Generalized Additive Models were used to explore nonlinear relationships, they were applied for explanatory rather than predictive purposes, so potential overfitting was not formally tested.

Regarding transferability, the identified meteorological thresholds (wind speed below 2 m s^{-1}, relative humidity below 65%, and high diurnal temperature range) and their nonlinear effects on PM concentrations are likely relevant to other urban areas in central Chile that share similar topographic confinement and winter stagnation patterns [34]. However, direct application of the current findings to other cities would require local calibration to account for differences in emission sources, basin geometry, and monitoring network characteristics.

5. Conclusions

This study provides a comprehensive evaluation of the Critical Episodes Management (CEM) system's performance in the Santiago Metropolitan Region from 2017 to 2022, revealing persistent deficiencies and clear pathways for improvement.

The Cassmassi-1 model for PM_{10} forecasting exhibited severe limitations: it failed to predict more than 50% of actual critical episodes each year, with false-alarm rates consistently exceeding 60%. Overall accuracy for "No Episode" conditions remained above 84%, but episode-detection accuracy ranged from 33.3% (2020) to 47.4% (2021), resulting in undeclared episodes of 52.6–66.7%.

In contrast, the WRF-Chem component for $PM_{2.5}$ achieved substantially better results, with episode prediction accuracies of 64.7% (2020), 72.2% (2021), and 84.2% (2022), global accuracies above 70–86%, and undeclared episodes reduced to 15.8–35.3%.

Analysis of ~1.2 million hourly records from high-quality stations (Independencia, Cerro Navia, Pudahuel, El Bosque) using Generalized Additive Models explained 60–75% of $PM_{2.5}$ variance and 55–70% of PM_{10} variance. Key nonlinear drivers included wind speeds below 2 m s^{-1} (dominant threshold effect, e.g., ~40% average $PM_{2.5}$ reduction from 1 to 3 m s^{-1} in Pudahuel), pronounced diurnal temperature ranges indicative of strong thermal inversions, and relative humidity below 65% (associated with 75% of undeclared cases). Wind speed showed the strongest negative Pearson correlations (−0.65 to −0.78 for $PM_{2.5}$; −0.58 to −0.72 for PM_{10}; all $p < 0.01$).

A total of 172 critical $PM_{2.5}$ events were observed (versus 48 declared), with the highest frequencies in July (39.0%) and June (35.5%), and the greatest incidence at western stations (Pudahuel: 39 PM_{10} and 15 $PM_{2.5}$ episodes; Cerro Navia: 38 and 12, respectively).

These quantitative findings confirm the system's structural vulnerabilities, including linear assumptions, inadequate representation of dynamic emissions (e.g., residential wood combustion), data gaps (100% loss at Quilicura and Cerrillos), and reliance on surface-based vertical stability estimates. In addition, our results demonstrate that nonlinear, threshold-aware approaches can substantially enhance predictive skill. The diagnostic evidence presented here demonstrates that current linear assumptions are insufficient. Future research should focus on developing and rigorously validating predictive frameworks that integrate the identified nonlinear meteorological precursors and on improving vertical profiling. Addressing these modeling gaps is a critical step toward improving alert reliability, reducing population exposure, and strengthening regulatory compliance during extreme air quality episodes.

https://doi.org/10.3390/su18083652

Supplementary Materials: The following supporting information can be downloaded at: https://www.mdpi.com/article/10.3390/su18083652/s1, Table S1: Contingency tables for the Cassmassi-1 model (PM_{10}) performance during the 2020–2022 winter periods (full four-category evaluation); Table S2: Contingency tables for the WRF-Chem model ($PM_{2.5}$) performance during the 2020–2022 winter periods (full four-category evaluation).

Author Contributions: Conceptualization, L.A.D.-R., M.O. and F.V.; methodology, L.A.D.-R., M.O., J.L., A.M., S.A.-M. and F.V.; software, M.O., J.L., A.M. and F.V.; validation, L.A.D.-R., M.O., J.L., A.M., R.Z., D.Y. and F.V.; formal analysis, L.A.D.-R., M.O., J.L., A.M., S.A.-M., R.Z. and F.V.; investigation, L.A.D.-R., M.O., J.L., A.M., S.A.-M., R.Z., D.Y., A.E.-P., L.E.-P., E.P.-C. and F.V.; resources, L.A.D.-R. and F.V.; data curation, M.O., J.L., A.M., S.A.-M. and F.V.; writing—original draft preparation, L.A.D.-R., M.O., J.L., A.M. and F.V.; writing—review and editing, L.A.D.-R., M.O., J.L., A.M., S.A.-M., R.Z., D.Y., A.E.-P., L.E.-P., E.P.-C. and F.V.; visualization, M.O., J.L., A.M. and F.V.; supervision, L.A.D.-R. and F.V.; project administration, L.A.D.-R. and F.V.; funding acquisition, F.V. All authors have read and agreed to the published version of the manuscript.

Funding: This research received no external funding.

Institutional Review Board Statement: Not applicable.

Informed Consent Statement: Not applicable.

Data Availability Statement: The raw hourly air quality ($PM_{2.5}$ and PM_{10} concentrations) and meteorological data (wind speed, wind direction, relative humidity, temperature) used in this study are publicly available from the 'Sistema de Información Nacional de Calidad del Aire' (SINCA) of the Chilean Ministry of the Environment. These data can be accessed and downloaded directly from the official SINCA portal at https://sinca.mma.gob.cl/ (accessed on 1 November 2025) for the relevant monitoring stations in the Santiago Metropolitan Region during the winter periods (May–August) from 2017 to 2022.

Acknowledgments: This study was partially supported by the supercomputing infrastructure at the NLHPC (ECM-02).

Conflicts of Interest: The authors declare no conflicts of interest.

References

1. Tavares, M.S.; Rodrigues, C.T.; de Menezes, S.L.S.; Moreno, A.M. Health at Risk: Air Pollution and Urban Vulnerability—Perspectives in Light of the 2030 Agenda. *Green Health* **2025**, *1*, 21. [CrossRef]
2. Orsetti, E.; Tollin, N.; Lehmann, M.; Valderrama, V.A.; Morató, J. Building Resilient Cities: Climate Change and Health Interlinkages in the Planning of Public Spaces. *Int. J. Environ. Res. Public Health* **2022**, *19*, 1355. [CrossRef] [PubMed]
3. Nagendra, H.; Bai, X.; Brondizio, E.S.; Lwasa, S. The Urban South and the Predicament of Global Sustainability. *Nat. Sustain.* **2018**, *1*, 341–349. [CrossRef]
4. Basoa, K.; Fleming, Z.L.; Leiva, M.A.; Concha, C.; Menares, C. Current Status, Trends, and Future Directions in Chilean Air Quality: A Data-Driven Perspective. *Atmosphere* **2025**, *16*, 733. [CrossRef]
5. Jorquera, H. Air Quality Management in Chile: Effectiveness of PM2.5 Regulations. *Urban Clim.* **2021**, *35*, 100764. [CrossRef]
6. Menares, C.; Perez, P.; Parraguez, S.; Fleming, Z.L. Forecasting PM2.5 Levels in Santiago de Chile Using Deep Learning Neural Networks. *Urban Clim.* **2021**, *38*, 100906. [CrossRef]
7. Langner, J.; Gidhagen, L.; Bergström, R.; Gramsch, E.; Oyola, P.; Reyes, F.; Segersson, D.; Aguilera, C. Model-Simulated Source Contributions to PM2.5 in Santiago and the Central Region of Chile. *Aerosol Air Qual. Res.* **2020**, *20*, 1111–1126. [CrossRef]
8. Muñoz, R.C.; Whiteman, C.D.; Garreaud, R.D.; Rutllant, J.A.; Hidalgo, J. Using Commercial Aircraft Meteorological Data to Assess the Heat Budget of the Convective Boundary Layer Over the Santiago Valley in Central Chile. *Bound. Layer Meteorol.* **2022**, *183*, 295–319. [CrossRef]
9. Lapere, R.; Menut, L.; Mailler, S.; Huneeus, N. Seasonal Variation in Atmospheric Pollutants Transport in Central Chile: Dynamics and Consequences. *Atmos. Chem. Phys.* **2021**, *21*, 6431–6454. [CrossRef]

10. Muñoz, R.C.; Corral, M.J. Surface Indices of Wind, Stability, and Turbulence at a Highly Polluted Urban Site in Santiago, Chile, and Their Relationship with Nocturnal Particulate Matter Concentrations. *Aerosol Air Qual. Res.* **2017**, *17*, 2780–2790. [CrossRef]
11. Álamos, N.; Huneeus, N.; Opazo, M.; Osses, M.; Puja, S.; Pantoja, N.; Denier van der Gon, H.; Schueftan, A.; Reyes, R.; Calvo, R. High-Resolution Inventory of Atmospheric Emissions from Transport, Industrial, Energy, Mining and Residential Activities in Chile. *Earth Syst. Sci. Data* **2022**, *14*, 361–379. [CrossRef]
12. Busch, P.; Cifuentes, L.A.; Cabrera, C. Chronic Exposure to Fine Particles (PM2.5) and Mortality: Evidence from Chile. *Environ. Epidemiol.* **2023**, *7*, e253. [CrossRef] [PubMed]
13. Pino-Cortés, E.; Díaz-Robles, L.A.; Campos, V.; Vallejo, F.; Cubillos, F.; Gómez, J.; Cereceda-Balic, F.; Fu, J.; Carrasco, S.; Figueroa, J. Effect of Socioeconomic Status on the Relationship Between Short-Term Exposure to PM2.5 and Cardiorespiratory Mortality and Morbidity in a Megacity: The Case of Santiago de Chile. *Air Qual. Atmos. Health* **2020**, *13*, 509–517. [CrossRef]
14. Mardones, C.; Cornejo, N. Ex-Post Evaluation of Environmental Decontamination Plans on Air Quality in Chilean Cities. *J. Environ. Manag.* **2020**, *256*, 109929. [CrossRef]
15. Richard Toro, A.; Tomás Claramunt, A.; Fiorella González, V.; Sebastián Ávila, G.; Manuel, A.L.G. Long-Term Assessment and Acute Air Pollution Events in a Mega-Industrial Area in Central Chile. *Urban Clim.* **2024**, *55*, 101880. [CrossRef]
16. Lapere, R.; Menut, L.; Mailler, S.; Huneeus, N. Soccer Games and Record-Breaking $PM_{2.5}$ Pollution Events in Santiago, Chile. *Atmos. Chem. Phys.* **2020**, *20*, 4681–4694. [CrossRef]
17. Morales, R.G.E.; Llanos, A.; Merino, M.; Gonzalez-Rojas, C.H. A Semi-Empirical Method of PM-10 Atmospheric Pollution Forecast at Santiago de Chile City. *Nat. Environ. Pollut. Technol.* **2012**, *11*, 181–186.
18. Grell, G.A.; Peckham, S.E.; Schmitz, R.; McKeen, S.A.; Frost, G.; Skamarock, W.C.; Eder, B. Fully Coupled "Online" Chemistry within the WRF Model. *Atmos. Environ.* **2005**, *39*, 6957–6975. [CrossRef]
19. Wood, S.N. *Generalized Additive Models: An Introduction with R*, 2nd ed.; Chapman and Hall/CRC: Boca Raton, FL, USA, 2017. [CrossRef]
20. Pearce, J.L.; Beringer, J.; Nicholls, N.; Hyndman, R.J.; Tapper, N.J. Quantifying the Influence of Local Meteorology on Air Quality Using Generalized Additive Models. *Atmos. Environ.* **2011**, *45*, 1328–1336. [CrossRef]
21. R CoreTeam. *R 2023 R: A Language and Environment for Statistical Computing*; v.4.3.2; R Foundation for Statistical Computing: Vienna, Austria, 2023. Available online: https://cran.r-project.org/bin/windows/base/old/4.3.2/ (accessed on 3 November 2023).
22. Muñoz, R.C.; Garreaud, R.; Rutllant, J.A.; Seguel, R.; Corral, M. New Observations of the Meteorological Conditions Associated with Particulate Matter Air Pollution Episodes in Santiago, Chile. *Atmosphere* **2023**, *14*, 1454. [CrossRef]
23. Chen, Z.; Chen, D.; Zhao, C.; Kwan, M.p.; Cai, J.; Zhuang, Y.; Zhao, B.; Wang, X.; Chen, B.; Yang, J.; et al. Influence of Meteorological Conditions on PM2.5 Concentrations Across China: A Review of Methodology and Mechanism. *Environ. Int.* **2020**, *139*, 105558. [CrossRef]
24. Lou, C.; Liu, H.; Li, Y.; Peng, Y.; Wang, J.; Dai, L. Relationships of Relative Humidity with PM2.5 and PM10 in the Yangtze River Delta, China. *Environ. Monit. Assess.* **2017**, *189*, 582. [CrossRef]
25. Morales-Solís, K.; Ahumada, H.; Rojas, J.P.; Urdanivia, F.R.; Catalán, F.; Claramunt, T.; Toro, R.A.; Manzano, C.A.; Leiva-Guzmán, M.A. The Effect of COVID-19 Lockdowns on the Air Pollution of Urban Areas of Central and Southern Chile. *Aerosol Air Qual. Res.* **2021**, *21*, 200677. [CrossRef]
26. Urrutia-Mosquera, J.A.; Flórez-Calderón, L.Á. Impact of Confinement on the Reduction of Pollution and Particulate Matter Concentrations. *Reflections for Public Transport Policies. Environ. Process.* **2022**, *10*, 2. [CrossRef]
27. Dales, R.; Blanco-Vidal, C.; Romero-Meza, R.; Schoen, S.; Lukina, A.; Cakmak, S. The Association between Air Pollution and COVID-19 Related Mortality in Santiago, Chile: A Daily Time Series Analysis. *Environ. Res.* **2021**, *198*, 111284. [CrossRef] [PubMed]
28. Salini, G.A.; Pacheco, P.R.; Mera, E.; Parodi, M.C. Probable Relationship between COVID-19, Pollutants and Meteorology: A Case Study at Santiago, Chile. *Aerosol Air Qual. Res.* **2021**, *21*, 200434. [CrossRef]
29. Pacheco, P.; Mera, E.; Navarro, G. The Effects of Lockdown, Urban Meteorology, Pollutants, and Anomalous Diffusion on the SARS-CoV-2 Pandemic in Santiago de Chile. *Atmosphere* **2024**, *15*, 414. [CrossRef]
30. Ruggeri, M.F.; Bolaño-Ortiz, T.; Cereceda-Balic, F. Atmospheric Black Carbon in a Key Location of the Chilean Central Andes: Identifying Patterns, Sources, and Potential Impacts. *Atmos. Environ.* **2024**, *318*, 120273. [CrossRef]
31. Zalakeviciute, R.; Lopez-Villada, J.; Ochoa, A.; Moreno, V.; Byun, A.; Proaño, E.; Mejía, D.; Bonilla-Bedoya, S.; Rybarczyk, Y.; Vallejo, F. Urban Air Pollution in the Global South: A Never-Ending Crisis? *Atmosphere* **2025**, *16*, 487. [CrossRef]
32. Puentes, R.; Marchant, C.; Leiva, V.; Figueroa-Zúñiga, J.I.; Ruggeri, F. Predicting PM2.5 and PM10 Levels during Critical Episodes Management in Santiago, Chile, with a Bivariate Birnbaum-Saunders Log-Linear Model. *Mathematics* **2021**, *9*, 645. [CrossRef]

33. Vallejo, F.; Villacrés, P.; Yánez, D.; Espinoza, L.; Bodero-Poveda, E.; Díaz-Robles, L.A.; Oyaneder, M.; Campos, V.; Palmay, P.; Cordovilla-Pérez, A.; et al. Prolonged Power Outages and Air Quality: Insights from Quito's 2023–2024 Energy Crisis. *Atmosphere* **2025**, *16*, 274. [CrossRef]
34. Vallejo, F.; Yánez, D.; Viñán-Guerrero, P.; Díaz-Robles, L.A.; Oyaneder, M.; Reinoso, N.; Billartello, L.; Espinoza-Pérez, A.; Espinoza-Pérez, L.; Pino-Cortés, E. Enhancing Air Quality Predictions in Chile: Integrating ARIMA and Artificial Neural Network Models for Quintero and Coyhaique Cities. *PLoS ONE* **2025**, *20*, e0314278. [CrossRef] [PubMed]